Rend. Fis. Acc. Lincei (2012) 23:121–129
DOI 10.1007/s12210-012-0166-4

Relative sea-level rise and marine erosion and inundation in the Sele river coastal plain (Southern Italy): scenarios for the next century

Gerardo Pappone · Pietro Patrizio Ciro Aucelli · Ines Aberico · Vincenzo Amato · Fabrizio Antonioli · Massimo Cesarano · Gianluigi Di Paola · Nicola Pelosi

Received: 14 December 2011 / Accepted: 12 January 2012 / Published online: 22 February 2012

Abstract In order to assess the effects of possible future sea-level rise in the Sele plain, the lowlands prone to inundation and the rate of coastal erosion in the years 2050 and 2100 have been discussed and some conclusions are here proposed. The sea level at these two dates was calculated as the combination of three components: response of Italian coastal zones to the past deglaciation, variations in ocean volume due to the global warming and vertical land movements. The morpho-stratigraphical data, chronologically supported by ^{14}C and by archeo-tephro-stratigraphical dating, have allowed the identification of paleo-sea levels of the upper Pleistocene and Holocene (Amato et al. 2011). Such paleo-sea levels compared with those of the tectonically stable areas (Lambeck et al. 2011), permitted the detection of the different vertical land movements in the study area. In particular, in the SE sector of the coastal plain, the Holocene paleo-sea levels are slightly higher (ca. 1–2 m). These values could be considered due to a gentle uplift of the area during Holocene times (0.22 mm/year). In the central sector of the plain, near the Sele river mouth and in the NW sector, between the Sele and Tusciano river mouths, the altitude of the Late Quaternary coastal and lagoonal deposits are slightly lower (ca. 2–3 m). These values could be related to a gentle subsidence of the area during the Holocene (0.4 mm/year). The sea level rise of 5.9 mm/year (IPCC 2007) and 14 mm/year (Rahmstorf 2007) was considered to represent the maximum trends in the ocean volume variation at global scale. The third component, the glacio-hydro-isostasy, was represented by the value of 0.44 mm/year identified by Lambeck et al. (2011) at the Sele plain. The sum of these three components allowed to identify three sea-level scenarios slightly different for the northern and the southern sector of Sele plain, with values ranging from 357 to 1,526 mm and from 307 to 1,424 mm, respectively. For each scenario a simple approach was used, mainly based on the topographic elevation analysis of study area, applied to identify the extension of possible areas of inundation. It corresponds to a minimum value of about 0.42 km^2 for the 2050 AD and a maximum value of 7.6 km^2 for the 2100. Furthermore, according to the methodology proposed by Davidson-Arnott (2005), also the beach erosion

This paper is an outcome of the FISR project VECTOR (Vulnerability of the Italian coastal area and marine ecosystem to Climate changes and their role in the Mediterranean carbon cycles), subproject VULCOST (vulnerability of coastal environments to climate changes) on: land sea interaction and costal changes in the Sele river plain, Campania.

G. Pappone (✉) · P. P. C. Aucelli
Dipartimento di Scienze per l'Ambiente, Centro direzionale, Università di Napoli Parthenope, isola c4, 80143 Napoli, Italy
e-mail: gerardo.pappone@uniparthenope.it

I. Aberico
Centro Interdipartimentale di Ricerca Ambiente, Università degli Studi "Federico II" di Napoli, Via Mezzocannone 16, 80134 Napoli, Italy

V. Amato · M. Cesarano · G. Di Paola
Dipartimento di Scienze e Tecnologie per l'Ambiente e il Territorio, Università del Molise, C.da Fonte Lappone, 86090 Pesche, IS, Italy

F. Antonioli
ENEA, Agenzia Nazionale per le Nuove Tecnologie, l'Energia e l'Ambiente, Via Anguillarese 301, 00060 S. Maria di Galeria, 00123 Rome, Italy

N. Pelosi
Istituto per l'Ambiente Marino Costiero, CNR, Calata Porta di Massa, 80133 Napoli, Italy

was evaluated. The computations showed a potential mean landward retreat of the shoreline ranging from 19 to 93 m.

Keywords Sele river coastal plain · Sea-level rise scenarios · Marine inundation hazard · Coastal erosion hazard

1 Introduction

The Sele coastal plain, located in the southern Campania Region (southern Italy) between the towns of Salerno and Agropoli (Fig. 1), is the result of the sedimentary aggradation in a Plio-Quaternary tectonic depression located along the western Tyrrhenian margin of the southern Apennine Chain (Cinque et al. 2009; Pappone et al. 2009).

The plain that extends over an area of about 400 km^2 is bounded seawards by a narrow sandy coastal strip and landwards by the Lattari and Picentini Mts. (on the N) and by the Cilento Mts. (on the SE). Further seawards, the coastal plain is characterized by an elongated beach dune ridge formed during the last Interglacial period (MIS 5, between 130 and 70 ky BP; Brancaccio et al. 1988), known as Gromola paleoridge (Cinque et al. 2009 and Fig. 1).

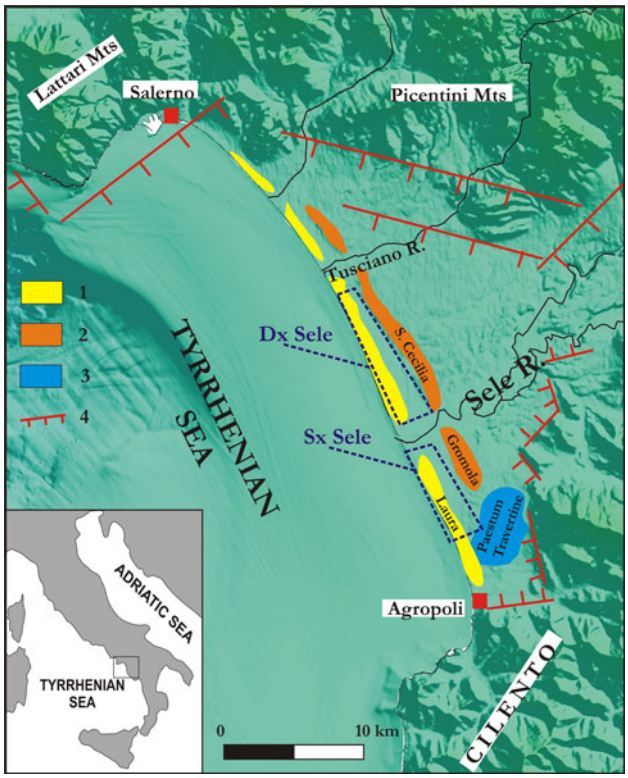

Fig. 1 Schematic map of the Sele Plain showing (*1*) the last Interglacial and (*2*) Holocene coastal ridges, (*3*) Paestum Travertines and (*4*) main normal faults (*barbs* indicate downthrown side). The *dashed rectangles* delineate the sectors of the plain (Dx and Sx Sele) where the boreholes with chrono-altimetrical markers, used for the vertical land component evaluation, are located

Close to the present coastline, a composite sandy ridge occurs representing the evolution of a Holocene barrier-lagoon system (Cinque et al. 2009; Pappone et al. 2009; Amato et al. 2011). It disappears inland under a flat, muddy, back dune depression. Moving from inland to the sea, the dune system shows at least three orders of paleoridges: Laura ridge dated from 5.3 to 3.6 ky BP, Sterpina I and Sterpina II ridges, dated, respectively, older than 2.6 ky BP and about 2 ky BP (Brancaccio et al. 1986 and 1988; Barra et al. 1998; and 1999). These sandy ridges constitute a discontinuous dune system with a mean height of about 3 m a.s.l interrupted by rivers and man-made drainage channels. The back-ridge depressions, only recently drained, are spread over a large area of the plain, with a mean height of about 0.50 m/1.5 m asl. The naturalness of the area is quite well preserved, but some sectors are influenced by human activity, critical since the 1950s (Alberico et al. 2011).

These main features point out the fragility of the study area to risks due to sea-level changes.

For the next century, the global sea level should rise at a maximum value of 59 cm according to IPCC (2007) and of about 140 cm, according to Rahmstorf (2007) in relation to the global model used. These values, the vertical land movements and the effects of past deglaciation, were quantified and summed to define the Relative Sea-level Rise (RSLR) for 2050 and 2100 AD at Sele Plain. Three different scenarios were identified and used to depict the areas that could be interested by coastal erosion and marine inundation.

A preliminary approach, mainly based on the topographic elevation analysis of study area, was used to define both the areas potentially subject to inundation (lowland zones close to the shoreline) and to erosion (shoreline retreat).

2 Sea-level change assessment

The relative sea-level change at Sele plain has been considered as the sum of the glacio-hydro-isostasy, the changes in ocean volume (eustatic) and the vertical land movements.

2.1 Glacio-hydro-isostasy

We used as glacio-isostatic component, the sea level predicted for the past 100 years for 40 sites (site 9 for Sele plain, Lambeck et al. 2011) located along the Italian coasts, since it could be considered as a tool to assess the relative

sea level in the next future. At Sele plain, the sea level is rising, as a consequence of past deglaciations, at a rate of 0.44 mm/years (see Table 1a, b).

2.2 Change in ocean volume

To consider the effects of the future change in oceans volume, caused by global warming and ice melting, we used the highest sea-level rise rates predictions. In particular, in our model, we have adopted a sea-level rise prediction for 2100 AD of 5.9 mm/year proposed in A1F1 IPCC (IPCC 2007) and of 14 mm/year proposed by Rahmstorf (2007).

2.3 Vertical land movements

The vertical land component was evaluated with a chronostratigraphic study, integrated by a detailed geomorphological analysis, based on cartographic (1:5,000 in scale) and photo-aerial interpretation. About 200 cores very close to the present day shoreline (dashed polygons in Fig. 1) were analyzed in the study area. The cores interpretation was supported by paleoecological/paleo-environmental (mollusks, ostracods, benthic foraminifera and pollens) and tephrostratigraphical analyses as well as by ^{14}C datings (Barra et al. 1998, 1999; Cinque et al. 2009; Amato et al. 2011), and according to Amato et al. (2011), different sedimentary units (dunal sands, beach sands, upper shoreface sands, lagoonal silts and clays, fluvial-marshy sands, silts and clays) were identified.

This approach allowed to recognize several horizons and biological events that were used as paleo-sea-level markers, well constrained by tephra layers (Amato et al. 2011) and by ^{14}C AMS datings (Barra et al. 1998 and 1999; Cinque et al. 2009; Amato et al. 2011).

The paleo-sea-level markers were first corrected taking into account the drilling and ecological-induced uncertainties (according to Lambeck et al. 2004) and then compared with the Holocene-predicted sea-level curve relative to the Sele plain (site n. 9 in Lambeck et al. 2011).

Differential uplift/subsidence trends into the plain were identified. The data set have been grouped into two sectors: the Dx Sele river (from the Sele mouth to the Tusciano mouth) and the Sx Sele river (from the Sele mouth to the

Table 1 Vertical component of the Dx Sele (a) and Sx Sele (b) in the predicted sea-level rise

No.	Font	Depth (m asl)	Marker	Radiocarbon age (year BP)	Cal BP age (ky BP)	Vertical movement (m)	Ground deformation rate (mm/year)	Average (mm/year)
a								
1	Barra et al. (1998)	−1.5	Lagoonal organic matter	1.555 ± 60	1.5–1.3	−0.8	−0.5	−0.4 mm/year
2	Barra et al. (1998)	−3	Lagoonal organic matter	3.400 ± 60	3.7–3.5	−0.7	−0.2	
3	Barra et al. (1998)	−6	Lagoonal organic matter	3.675 ± 65	4.1–3.9	−3.3	−0.82	
4	Barra et al. (1998)	−4	Lagoonal organic matter	4.140 ± 65	4.8–4.5	−0.6	−0.13	
5	Barra et al. (1998)	−1	Lagoonal organic matter	5.535 ± 70	6.4–6.3	+5	+0.78	+0.8 mm/year
6	Barra et al. (1999)	−7	Lagoonal organic matter	6.530 ± 70	7.5–7.4	−1	−0.13	
7	Barra et al. (1999)	−6	Lagoonal organic matter	7.050 ± 80	7.9–7.8	+8	+1	
8	Barra et al., (1999)	−8.8	Lagoonal organic matter	7.360 ± 75	8.3–8.1	+1.2	+0.14	
9	Barra et al. (1998)	−6.5	Lagoonal organic matter	8.090 ± 90	9.2–8.8	+22.5	+2.5	
10	Barra et al. (1999)	−16	Lagoonal organic matter	8.300 ± 80	9.4–9.2	+13	+0.8	
11	Barra et al. (1998)	−8	Lagoonal organic matter	8.340 ± 90	9.4–9.2	+21	+2.25	
b								
1	Amato et al. (2011)	−0.9	Ceramic remains into lagoon		2.6–2.5	+0.5	+0.2	+0.22 mm/year
2	Amato et al. (2011)	−1.75	AMS tephra into lagoon		4.1	+1	+0.24	
3	Amato et al. (2011)	−7	Cerastoderma glaucum		7.0–6.7	+1.2	+0.17	+0.65 mm/year
4	Amato et al. (2011)	−8	Ammonia tepida		7.2–7.1	+2	+0.27	
5	Amato et al. (2011)	−10.5	Cerastoderma glaucum		7.9–7.7	+3	+0.38	
6	Barra et al. (1999)	−4	Lagoonal organic clay	7.140 ± 80	8.0–7.9	+10	+1.25	
7	Barra et al. (1999)	−12	Lagoonal organic clay	9.170 ± 90	10.4–10.2	+32	+3.2	+3.05 mm/year
8	Barra et al. (1999)	−20	Lagoonal organic clay	9.580 ± 100	11.1–10.8	+32	+2.90	

From left, the rows show the sample number, the references, the paleo-sea level markers, the conventional radiocarbon age, the calibrated radiocarbon age and the archeological and tephro-chronological data, the vertical movement compared to chrono-altimetrical data of the tectonically stable areas (Lambeck et al. 2011), the ground deformation rate (mm/year) and the average data sets

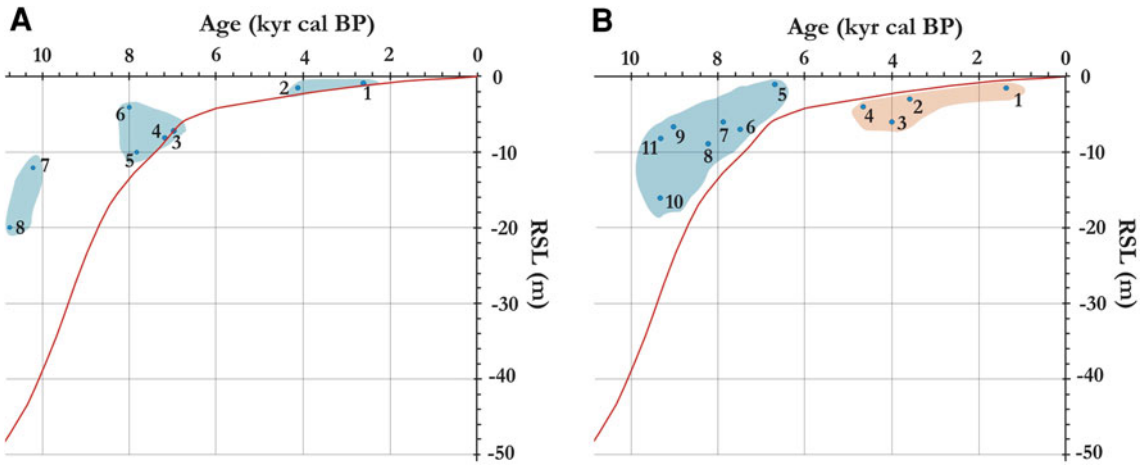

Fig. 2 Comparison between the observed relative sea-level data in the Dx Sele (**a**) and in the Sx Sele (**b**) sector, with their vertical uncertainties, and the Versilia (northern Tyrrhenian coast) predicted sea-level curve (redrawn after Lambeck et al. 2011). In *blue*, the positive values in meters (showing uplift), and in *orange*, the negative values (showing subsidence)

Paestum archeological area, Figs. 1, 2b; Table 1b). For each of these two areas, the long-term vertical movements were evaluated.

For the Dx Sele, our data suggest two trends: an uplift with an average rate of ca. 0,8 mm/year, from ca. 10 ky BP to ca. 6.0 ky BP, and a subsidence with an average rate of ca. 0,4 mm/year, from ca. 5.0 ky BP to ca.1.0 ky BP.

For the Sx Sele, our data showed an uplift trend with an average of 3.5 mm/year; at ca. 11–10 ky BP, of 0.65 mm/year at ca. 8.0–7.0 ky BP, and an average of 0.2 mm/year at ca. 4.0–2.5 ky BP.

Therefore, the data allowed us to identify an uplift of the whole Sele plain during the first part of the Holocene (up to ca. 6.0 ky BP) and a subsequent different behavior in the two sectors. The different vertical land movements into the plain seem to continue until to the present days, as evidenced by Vilardo et al. (2009), with geodetic data derived by PS-InSar interpretation (1992–2001 time period).

In order to evaluate the future sea-level rise, two different values of vertical land movements were considered: −0.82 mm/year for the Dx Sele and +0.2 mm/year for the Sx Sele. These values represent the highest ones recorded in the plain in the last 5 ky, and they must be regarded with caution, considering that the main values for −0.4 mm/year and +0.22 mm/year for Dx and Sx sectors, respectively, of the Sele plain.

2.4 Sea-level rise scenarios

The zones of Sele coastal plain that could be hit by marine inundation and coastal erosion in the years 2050 (time window of 50 years) and 2100 AD (time window of 100 years) were identified by using three possible scenarios of RSLR labeled with letter from A to C (Table 2a, b). These future events were defined as the concourse of the three components (glacio-hydro-isostasy, changes in ocean volume and vertical land movements), described in the previous paragraph.

The scenario "A" defined for the years 2050 is the outcome of a sea-level rise of 5.9 mm/year (scenario A1F1,

Table 2 Sea-level rise scenarios in the years 2050 and 2100 for Dx Sele (a) and Sx Sele (b)

	Year	SLR		Ground deformation rates		Glacio-hydro-isostasy		RSLR DX SELE
		mm/year	mm	mm/year (max)	mm (max)	mm/year	mm	mm (max)
a								
A	2050	5.9	295	−0.82	41	0.44	21.9	357
B	2100	5.9	590	−0.82	82	0.44	43.8	716
C	2100	14	1,400	−0.82	82	0.44	43.8	1,526
b								
A	2050	5.9	295	0.2	−10	0.44	21.9	307
B	2100	5.9	590	0.2	−20	0.44	43.8	614
C	2100	14	1,400	0.2	−20	0.44	43.8	1,424

IPCC 2007). The scenario "B" is identical to the scenario A, except that the time window considered is of 100 years. The scenario "C" is characterized by a sea-level rise of 14 mm/year (Rahmstorf 2007) and a time window of 100 years.

3 Marine inundation assessment

The potentially flooded zones were evaluated with a static model based on the comparison of Land Digital Elevation Model, (LDEM) and sea level in 2050 AD and 2100 AD (Mazria and Kershner 2007; Poulter and Halpin 2007; Rowley et al. 2007). The zones with the sea level exceeding the underlying ground surface elevation were identified as inundation-prone. We considered also the effect of the LDEM mean square error (± 0.5 m, see paragraph 4.1) on the inundation areas assessment; in fact, each flood area was delineated three times, considering three conditions: morphology of the study area, corresponding to: (a) the LDEM; (b) the LDEM minus 0.5 m and (c) the LDEM plus 0.5 m.

3.1 Land digital elevation model

The LDEM was defined by using the topographic data (elevation points and contour lines) of the Technical Map of the Campania Region, at scale 1:5,000, published in 2001. The study area encompasses the topographic height from 0 to 25 m asl. It represents, in fact, the zone exposed in the next future to potential erosion and/or inundation, caused by sea-level changes (Gornitz et al. 1982; IPCC 2007; Lambeck et al. 2011).

The procedure used to obtain the LDEM is based on the exploration of the elevation data to search for blunder, systematic and random errors. The blunder errors, that are the points with very high or very low values respect to the average elevation range of the study area (USGS 1997), were easily recognized and removed by selecting the points with values outside the elevation range (0–25 m) typical of the onshore coastal area. The systematic errors instead were not easily detectable (Brown and Bara 1994; Carter et al. 1994), because they mainly correspond to irrigation networks and are probably due to an erroneous registration of elevation of these artefacts in the contour line layers. To remove them, all points located within a distance of 5 m from both sides of irrigation network and irrigation lines have been selected and eliminated. The elimination of the random errors was complicated because their elevation only slightly differs from the adjacent points (USGS 1997). These errors were identified by using their distribution on the map of the elevation points, plotted in a distribution diagram available in the Geostatistical Analyst Module of

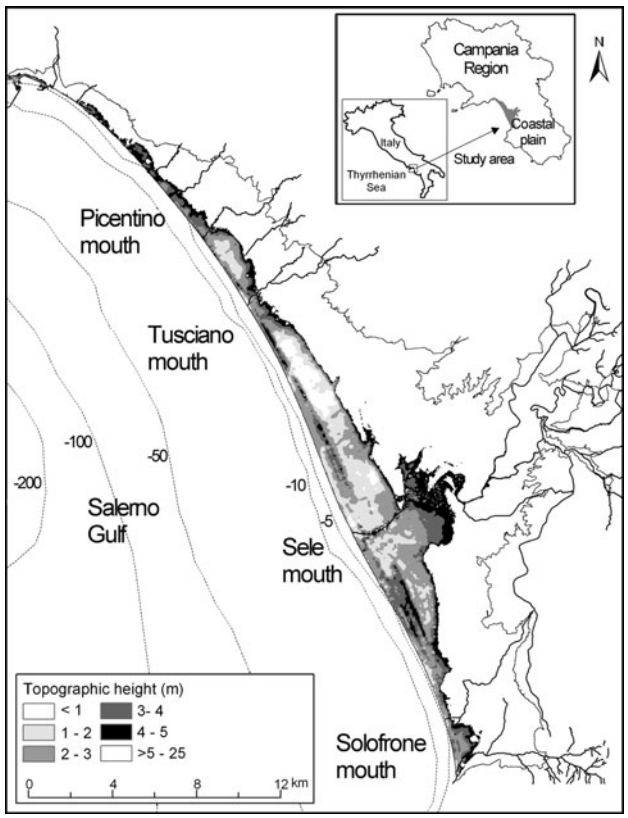

Fig. 3 Digital Elevation Model of onshore Sele coastal plain from the Picentino to the Solofrone river mouths

ArcGis software. Selecting each bar of the histogram, it has been possible to control if the data on a map are isolated points or groups of points. In the first case, the points were eliminated, in the second were preserved, but only if they represented local variation in morphology. Eliminated the spurious elevation points, by using the Kriging interpolation method, the LDEM of the Sele plain coastal area was generated (Fig. 3).

This raster model has a 10-m cell size and a mean square error of ±0.26 m, defined by using a cross-validation method (Liu et al. 2009; Wise 2011). External-validation was also carried out comparing the elevation values of 23 Regional and IGM vertices, falling inside the study area, with the interpolated elevation values extracted by the LDEM for the same points. This analysis highlighted a mean square error of ±0.54 m.

3.2 Marine inundation map

The lowlands of Sele coastal plain that will be hit by marine inundation in the years 2050 AD and 2100 AD were identified by using three scenarios of RSLR, labeled with letter from A to C (Table 2a, b).

In this preliminary study, the susceptibility of Sele coastal plain to inundation events was oversimplified and

mainly based on the topographic height analysis. The LDEM shown in Fig. 4 highlights a dune system characterized by a mean topographic height of about 3 m asl, where only a few dune crests reach 5 m in height, and a large back dune areas with a topographic height ranging from 0.5 to 1.5 m asl.

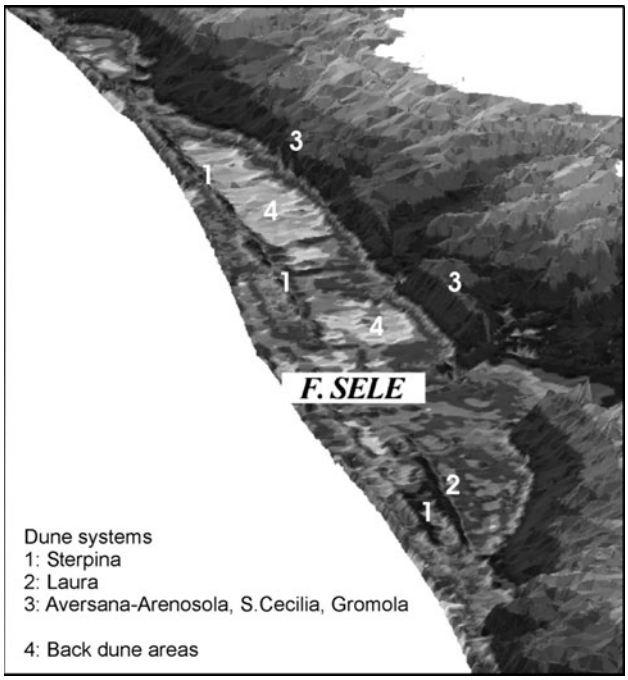

Fig. 4 3D visualization of the Sele coastal plain

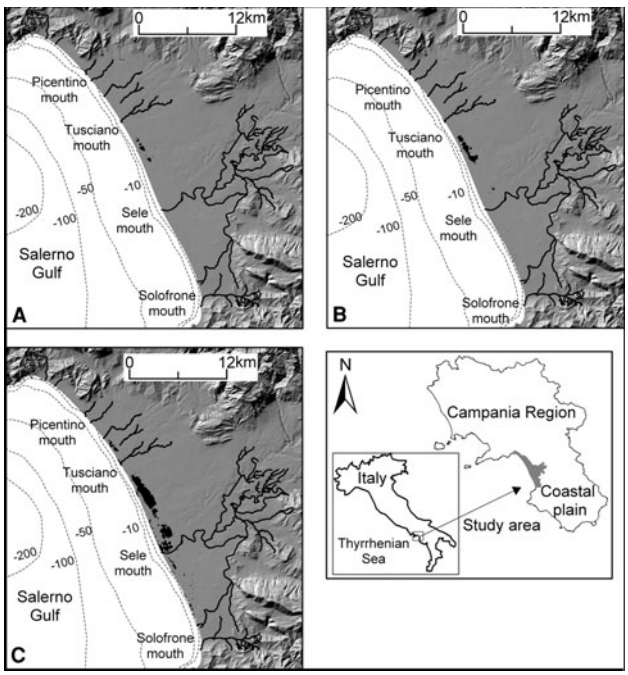

Fig. 5 Inundation susceptibility in the **a**, **b** and **c** scenarios, according to the LDEM. *Black areas* are inundable coastal sectors

These last zones have the highest probability to be inundated because of their topographic height and the discontinuities in the dune system.

The extension of areas susceptible to inundation is related to the sea-level scenarios identified in this paper with letters "A", "B" and "C", and to the effect of the LDEM mean square error.

The extension of inundated areas (Fig. 5; Table 3) increases from scenario A (ca. 2 km^2) to C (ca. 18 km^2) because the scenario "A" corresponds to the shortest time windows (50 years) considered, while the scenarios "B" and "C" are related to the longest time interval (100 years) and to the different values of RSLR due to global warming. The last scenario foresees the highest potential sea-level rise in Sele plain.

Finally, the same maps were drawn taking into account the effect of the mean square error of ±0.5 m in the LDEM. In particular, the maps of the Figs. 6, 7 were drawn considering the error –0.5 m (hereafter LDEM$^-$) and of +0.5 m (hereafter LDEM$^+$), respectively.

Table 3 Extension (in km^2) of lowland areas prone to inundation

Sea-level scenario	Land prone to inundation (km^2)		
	LDEM	LDEM$^+$	LDEM$^-$
A	0.4	0	2.3
B	1.6	0	4.5
C	7.6	3.2	16

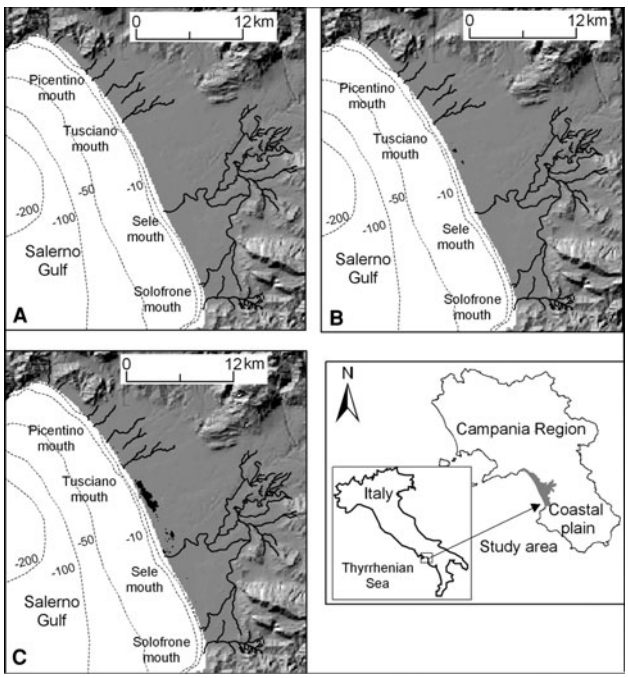

Fig. 6 Inundation susceptibility for **a**, **b** and **c** scenarios, considering a topographic model affected by a mean standard error of +50 cm (LDEM$^+$). *Black areas* are inundable coastal sectors

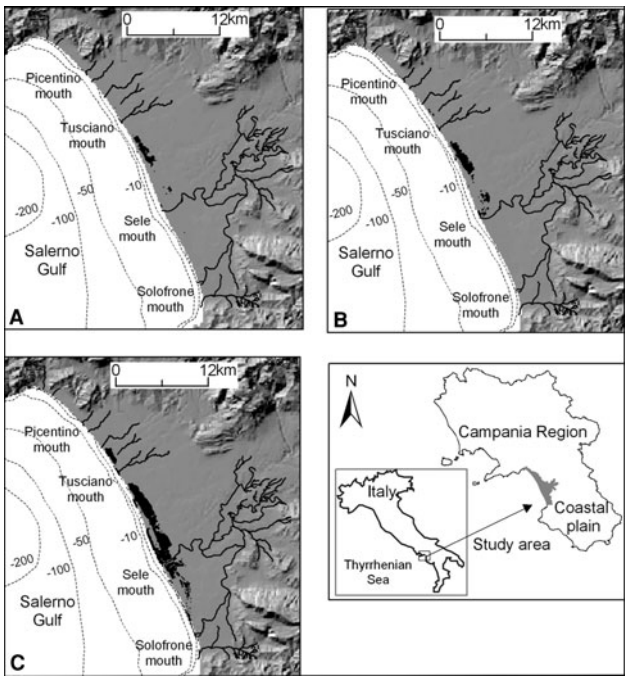

Fig. 7 Inundation susceptibility for **a**, **b** and **c** scenarios, considering a topographic model affected by a mean standard error of −50 cm (LDEM^{-}). *Black areas* are inundable coastal sectors

For the mean square error −0.5 m, the extension of inundated zones is the widest of the study area for all three scenarios (Table 3), while with a mean square error of +0.5 m, the scenarios A1 and B1 do not show inundation zones except for the C1 scenario.

4 Coastal erosion

In order to predict the effects of the sea-level rise on the Sele Plain shoreline, profiles of eight beaches from the Tusciano river mouth to the Agropoli promontory (Fig. 8) were realized by using a DGPS survey (Di Paola 2011). Along these profiles, the Davidson-Arnott (2005) flooding methods were used to estimate the probable coastal retreats (Table 4). This methodology differs from the classical Bruun rule (Bruun 1962). The hypotheses of Davidson-Arnott (2005) are as follows:

- The beach and foredune are eroded as a result of the profile modification because of sea-level rise, while the junction between the beach and the dune migrates landwards and upwards to keep pace with the rising sea level.
- A net onshore migration of sediment in the nearshore profile keeps pace with rising sea level. The outer part of the nearshore is eroded, and the point of closure moves landwards and upwards to keep pace with sea-level rise and with the landward migration of the shoreline.

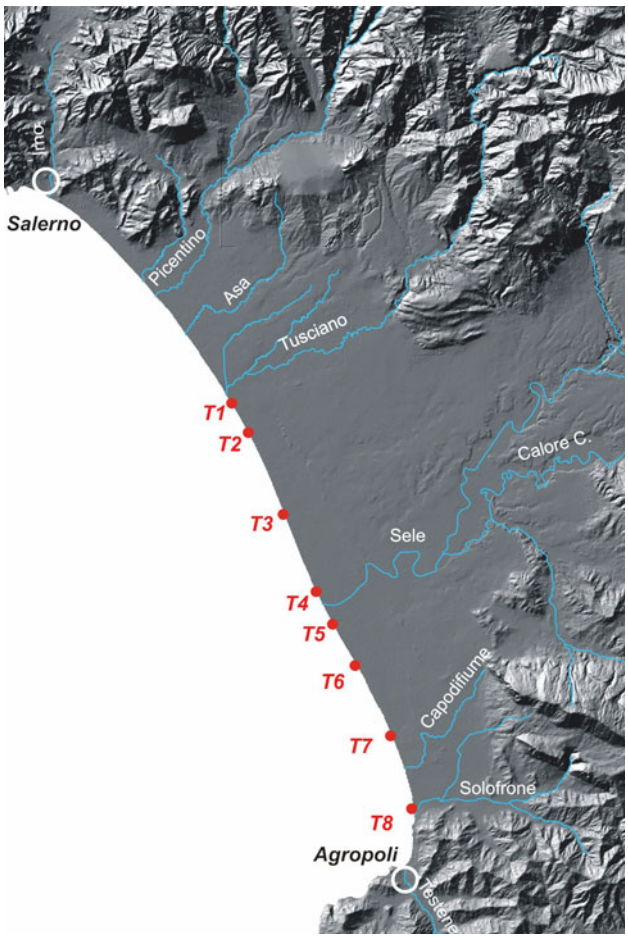

Fig. 8 Location of topographic profiles along the Sele coastline

Table 4 Amount of coastal retreat in the Sx and Dx Sele, applying the Flooding methodology of Davidson-Arnott (2005), which can be related to the scenarios showed in Fig. 6

Scenarios	Dx Sele plain		Sx Sele plain	
	m	m/year	m	m/year
A	19.30 ± 4.41	0.39	20.01 ± 2.46	0.40
B	38.71 ± 8.85	0.39	40.02 ± 4.92	0.40
C	82.50 ± 18.85	0.83	92.82 ± 11.41	0.93

- All the sediments eroded from the dune are transferred landwards, and as a consequence, the foredune migrates inland. Because the volume transferred landwards is equal to the volume eroded, the dune will maintain its overall volume.

This model allows the displacement of the shoreline to be independent from the actual shape of the beach profile and thus, whether the bars are present or not (Allison and Schwartz 1981), the displacement depends only from the tan β as follow:

$$R = S \cdot \frac{1}{\tan \beta}$$

where R is the shoreline retreat, S is the RSLR and β the slope of the profile between the dune ridge and the closure depth. The RSLR of scenarios "A," "B" and "C" was used to derive the mean retreat for the left and right side of Sele river (Table 4).

The predicted beach erosion shows a mean landward retreat of the shoreline of about 20 m for the 2050 AD (scenario "A") and of 40 m for the year 2100 AD (scenario "B"). However, in the scenario "C," adopting Rahmstorf (2007) prediction, the landward retreat could reach up to 93 m.

The method was based on a static approach; however, these predictions can be even worse in the case of incoming natural (i.e. extreme storms) or man-induced (i.e. deficit of coastal sediment supply) events.

5 Conclusions

The response of Sele coastal zone to the ongoing changes in ocean volume due to climatic changes combined with the vertical land movement and the glacio-hydro-isostasy has been here evaluated.

The comparison of the Holocene paleo-sea levels with those of the tectonically stable areas (sensu Lambeck et al. 2011) allowed to identify, during the Holocene, a gently uplifting in the SE sector of the coastal plain, with an average of 0.22 mm/year, and a subsidence for the sector between the Sele and Tusciano river mouths, with an average of −0.4 mm/year. In this work, we have used the highest rates of vertical movements corresponding to –0.82 mm/year for the Dx Sele and +0.2 mm/year for the Sx Sele (Table 1a, b).

These values, combined with the sea-level rise predictions (IPCC 2007; Rahmstorf 2007), due to global warming and the local effects of the glacio-hydro-isostasy (Lambeck et al. 2011), have allowed to identify three sea-level rise scenarios.

The use of a simple static inundation model allowed to identify the lowland areas that could be inundated. The extension of these areas ranges from a minimum of 0.42 $km^{2,}$ for the 2050 AD, to a maximum of 7.6 km^2 for the 2100 AD. In particular, these areas are mainly concentrated in the NW sector of Sele Plain, where the back-ridge zones are characterized by topographic elevation lower than 2 m above asl and should be considered as the major flood prone areas in the plain. Furthermore, because the extension of areas prone to inundation were demonstrated sensitive to the error associated to the DEM of Sele coastal zone, in the future, a more detailed study, based on a DEM with higher resolution, is necessary.

Moreover, it is important to consider that major historical earthquakes can cause very rapid coseismic vertical displacements (i.e. described in Mastronuzzi and Sansò 2002), and their effect can produce vertical movement over a time windows of different years constituting the primary cause of coastal flooding (Ballu et al. 2011).

The coastal retreat, due to sea-level rise predicted for the years 2050 and 2100 AD, was also calculated, according to the flooding method (Davidson-Arnott 2005). In this case, the mean retreat values vary from a minimum of ca 19 m to a maximum of ca 93 m. In the latter case, the landward retreat of the coastline could be very severe for the future dune ridge preservation, since the mean width of the present backshore does not exceed 80 m.

Finally, this study shows a high sensitivity of the Sele plain to the future RSLR, particularly in the NW sector, where the back-ridge area, characterized by a less elevated and flat morphology, could undergo major flood risks respect to the SE sector. The above geologic hazard needs to be carefully taken into account in the future management of this territory.

References

Alberico I, Amato V, Aucelli PPC, D'Argenio B, Di Paola G, Pappone G (2011) Historical shoreline evolution and recent shoreline trends of Sele Plain coastline (Southern Italy). The 1870–2009 time window. J Coastal Res. doi:10.2112/JCOASTRES-D-10-00197

Allison H, Schwartz ML (1981) The Bruun rule—the relationship of sea level change to coastal erosion and deposition. Proc R Soc Vic 93:87–97

Amato V, Aucelli PPC, Cinque A, D'Argenio B, Di Donato V, Russo Ermolli E, Pappone G, Petrosino P, Rosskopf CM et al (2011) Holocene palaeo-geographical evolution of the Sele river coastal plain (Southern Italy): new morpho-sedimentary data from the Paestum area. Il Quaternario 24:5–7

Ballu V, Bouin M-N, Siméoni P (2011) Comparing the role of absolute sea-level rise and vertical tectonic motions in coastal flooding, Torres Islands (Vanuatu). Proc Natl Acad Sci 108(32): 13019–13022

Barra D, Calderoni G, Cinque A, De Vita P, Rosskopf C, Russo Ermolli E et al (1998) New data on the evolution of the Sele river coastal plain (Southern Italy) during the Holocene. Il Quaternario 11(2):287–299

Barra D, Calderoni G, Cipriani M, De La Geniere J, Fiorillo L, Greco G, Mariotti Lippi M, Mori Secci M, Pescatore T, Russo B, Senatore MR, Tocco Sciarelli G, Thorez J et al (1999) Depositional history and palaeogeographic reconstruction of Sele coastal plain during Magna Grecia settlement of Hera Argiva (Southern Italy). Geologica Romana 35:151–166

Brancaccio L, Cinque A, Belluomini G, Branca M, Delitalia L (1986) Isoleucine Epimerization dating and tectonic significante of Upper Pleistocene sea-level features of the Sele Plain (Southern Italy). Z Geomorph NF Suppl.-Bd. 62:159–166

Brancaccio L, Cinque A, Russo F, Santangelo N, Alessio M, Allegri L, Improta S, Belluomini G, Branca M, Delitalia L (1988) Nuovi dati cronologici sui depositi marini e continentali della Piana del F. Sele e della costa settentrionale del Cilento (Campania, Appennino Meridionale). Atti del 74° Congresso della. Soc Geol It A:55–66

Brown DG, Bara TJ (1994) Recognition and reduction of systematic error in elevation and derivative surfaces from TI/2-minute DEMs. Photogramm Eng Remote Sens 60(2):189–194

Bruun P (1962) Sea-level rise as a cause of shore erosion. J Waterways Harbours Div 88(1–3):117–130

Carter TR, Parry ML, Nishioka S, Harasawa H (1994) Technical guidelines for assessing climate change impacts and adaptation. University College London and Centre for Global Environmental Research, Tskuba

Cinque A, Romano P, Budillon F, D'Argenio B (2009) Note illustrative della carta geologica d'Italia 1:50,000, Foglio 486, Salerno—ISPRA, Roma

Davidson-Arnott RGD (2005) A conceptual model of the effects of sea level rise on sandy coasts. J Coastal Res 21(6):1166–1172

Di Paola G (2011) Geological and geo-morphological characterization of coastal Sele plain (Campania, Italy) and considerations about its vulnerability. PhD Thesis, Università degli Studi del Molise, Italy. URL: http://road.unimol.it/handle/2192/141

Gornitz V, Lebedeff S, Hansen J (1982) Global sea level trend in the past century. Science 215:1611–1614

IPCC (2007) Fourth assessment report—climate change 2007. Intergovernmental panel on climate change. Cambridge University Press, Cambridge

Lambeck K, Antonioli F, Purcell A, Silenzi S (2004) Sea level change along the Italian coast for the past 10,000 years. Quat Sci Rev 23:1567–1598

Lambeck K, Antonioli F, Anzidei M, Ferranti L, Leoni G, Scicchitano G, Silenzi S (2011) Sea level change along the Italian coast during the Holocene and projections for the future. Quat Int 232:250–257

Liu X, Zhang Z, Peterson J (2009) Evaluation of the performance of DEM interpolation algorithms for LiDAR data. In: Ostendorf B, Baldock P, Bruce D, Burdett M, Corcoran P (eds) Proceedings of the surveying & spatial sciences institute biennial international conference, Adelaide, pp 771–780. ISBN: 978-0-9581366-8-6

Mastronuzzi G, Sansò P (2002) Holocene uplift rates and historical rapid sea-level changes at the Gargano promontory, Italy. J Quat Sci 17(5–6):593–606

Mazria E, Kershner K (2007) Nation under siege: sea level rise at our doorstep. The 2030 Research Center, 2030, Inc./Architecture 2030, 34p. URL: http://www.architecture2030.org/pdfs/nation_under_siege.pdf

Pappone G, Casciello E, Cesarano M, D'Argenio B, Conforti A (2009) Note illustrative della carta geologica d'Italia 1:50,000, Foglio 467, Salerno—ISPRA, Roma

Poulter B, Halpin PN (2007) Raster modelling of coastal flooding from sea-level rise. Int J Geograph Inform Sci 22(2):167–182

Rahmstorf S (2007) A semi-empirical approach to projecting future sea-level rise. Science 315:368–370

Rowley RJ, Kostelnick JC, Braaten D, Li X, Meisel J (2007) Risk of rising sea level to population and land area. Eos Trans Am Geophys Union 88(9):105–107

USGS (1997) Draft content standards for digital elevation model. Subcommittee on base cartographic data, Federal Geographic data committee

Vilardo G, Ventura G, Terranova C, Matano F, Nardò S (2009) Ground deformation due to tectonic, hydrothermal, gravity, hydrogeological, and anthropic processes in the Campania Region (Southern Italy) from permanent Scatterers synthetic aperture radar interferometry. Remote Sens Environ 113:197–212

Wise S (2011) Cross-validation as a means of investigating DEM interpolation error. Comput Geosci 37:978–991